Original Article

Rapid Turnover of Phosphatidylinositol-4,5-Bisphosphate in Insulin-Secreting Cells Mediated by Ca^{2+} and the ATP-to-ADP Ratio

Sophia Thore, Anne Wuttke, and Anders Tengholm

Phosphatidylinositol-4,5-bisphosphate (PIP_2) is important for a variety of cellular processes as a precursor for second messengers and by regulating ion channels, the cytoskeleton, and vesicle traffic in many types of cells, including insulin-secreting β-cells. Here, we applied evanescent wave microscopy and the PIP_2-binding pleckstrin homology domain from phospholipase C (PLC)-δ fused to the green fluorescent protein to characterize the regulation of plasma membrane PIP_2 in individual insulin-secreting MIN6 β-cells. Elevation of the glucose concentration from 3 to 11 mmol/l evoked antisynchronous oscillations of [PIP_2] and cytoplasmic Ca^{2+}concentration, consistent with PLC being periodically activated by the voltage-dependent Ca^{2+} influx. The effect of adenine nucleotides on [PIP_2] was studied in cells permeabilized with α-toxin. ATP dose-dependently stimulated PIP_2 synthesis with half-maximal effect at 300 μmol/l. Omission of the nucleotide resulted in rapid loss of PIP_2 with $t_{1/2}$ < 40 s. ADP also stimulated PIP_2 formation, but this effect reflected local ATP formation and was prevented by the adenylate kinase inhibitor diadenosine-pentaphosphate. The ATP-induced PIP_2 synthesis was counteracted by the ADP analog adenosine-5′-*O*-2-thiodiphosphate. We conclude that plasma membrane PIP_2 is dynamically regulated by intracellular Ca^{2+} and the ATP-to-ADP ratio in insulin-secreting cells. The rapid turnover allows maintenance of PIP_2 levels while generating second messengers of critical importance for insulin secretion. *Diabetes* 56:818–826, 2007

Phosphatidylinositol 4,5-bisphosphate (PIP_2) is a minor membrane component of eukaryotic cells constituting ~1% of the phospholipids in the inner leaflet of the plasma membrane. Nevertheless, the phospholipid plays important roles in the regulation of a variety of cell functions. Apart from serving as a precursor for the messenger molecules inositol-1,4,5-trisphosphate (IP_3) and diacylglycerol generated on activation of phospholipase C (PLC) (1), and for phosphoinositide 3-kinase–generated phosphatidylinositol-3,4,5-trisphosphate (2), PIP_2 is known to regulate ion channel activity (3), proteins involved in organization of the cytoskeleton (4), and the trafficking of vesicles in endo- and exocytosis (5). PIP_2 is mainly synthesized in two steps by phosphorylation of phosphatidylinositol to phosphatidylinositol-4-phosphate (PIP) by phosphatidylinositol 4-kinases (PI 4-kinases), followed by PIP phosphorylation to PIP_2 by type I PIP 5-kinases (6). Some PIP_2 is also formed via phosphorylation of phosphatidylinositol-5-phosphate by type II PIP 4-kinases (6).

Pancreatic β-cells secrete insulin after elevation of the ambient glucose concentration. The rapid uptake and metabolism of the glucose lead to an increase of the intracellular ATP-to-ADP ratio, closure of ATP-sensitive K^+ channels (K_{ATP} channels) in the plasma membrane, depolarization, and opening of voltage-dependent Ca^{2+} channels. The resulting increase of the cytoplasmic Ca^{2+} concentration ($[Ca^{2+}]_i$) triggers exocytosis of insulin secretory granules (7). A large amount of data indicates that PIP_2 plays an important role in the insulin secretory process. It was recognized early that the rate of phosphoinositide metabolism is increased in glucose-stimulated islets (8,9). This effect is due to PLC-mediated hydrolysis of PIP_2 (10). However, there are different opinions about the mechanisms underlying glucose-induced PLC activation. Whereas several studies indicate that the glucose-induced phosphoinositide hydrolysis depends on the presence of extracellular Ca^{2+} (9,11,12), other reports indicate that the process is at least in part Ca^{2+} independent (13–15). Recent observations in single insulinoma cells (16) and intact mouse islets (17) have demonstrated that elevation of $[Ca^{2+}]_i$ is sufficient to trigger PLC activity and that $[Ca^{2+}]_i$ oscillations are associated with periodic activation of PLC. However, the kinetics of the early changes in PIP_2 concentration and how it is related to $[Ca^{2+}]_i$ after glucose stimulation are unknown.

PIP_2 has been found to be important for secretion independent of its role as substrate for PLC. A role for PIP_2 in exocytosis was first suggested by the observation that phosphatidylinositol transfer protein and a type I PIP 5-kinase are essential components of the ATP-dependent priming of exocytotic vesicles in permeabilized chromaffin cells (18,19). The importance of PIP_2 was later confirmed by experiments showing that exocytosis is negatively affected by inhibition of PIP_2 synthesis in various types of cells (20,21), including insulin-secreting cells (22,23), and by the demonstration that exocytosis is inhibited by

From the Department of Medical Cell Biology, Uppsala University, Uppsala, Sweden.

Address correspondence and reprint requests to Anders Tengholm, Department of Medical Cell Biology, Uppsala University, Biomedical Centre, Box 571, SE-75123 Uppsala, Sweden. E-mail: anders.tengholm@mcb.uu.se.

Received for publication 21 June 2006 and accepted in revised form 27 November 2006.

ADPβS, adenosine-5′-*O*-2-thiodiphosphate; $[Ca^{2+}]_i$, cytoplasmic Ca^{2+} concentration; GFP, green fluorescent protein; IP_3, inositol-1,4,5-trisphosphate; K_{ATP} channel, ATP-sensitive K^+ channel; PH, pleckstrin homology; PI 4-kinase, phosphatidylinositol 4-kinase; PIP, phosphatidylinositol-4-phosphate; PIP_2, phosphatidylinositol-4,5-bisphosphate; PLC, phospholipase C.

DOI: 10.2337/db06-0843

overexpression of a PIP_2-binding protein domain (22,24). Moreover, it was recently shown that PIP_2 directly facilitates exocytosis in mouse β-cells (25), probably by mediating the ATP-dependent priming of vesicles. PIP_2 can also be expected to influence β-cell secretion via modulation of K_{ATP} channels (26) or the actin cytoskeleton as in other types of cells (27).

Despite the undisputed importance of PIP_2 for insulin release, little is known about the dynamics of the lipid in the plasma membrane of insulin-secreting cells. So far, most studies have employed conventional isotopic labeling methods, which typically provide poor time resolution and average responses from large numbers of cells. In the present study, we used an online imaging approach to selectively measure the PIP_2 concentration in the plasma membrane of individual insulin-secreting cells. The aims were to clarify how glucose affects membrane PIP_2 concentration, the relationship between changes in PIP_2 and $[Ca^{2+}]_i$, and how plasma membrane PIP_2 synthesis is regulated by the intracellular concentrations of ATP and ADP.

RESEARCH DESIGN AND METHODS

Plasmid constructs. Plasmids encoding the fusion constructs between the pleckstrin homology (PH) domain of PLCδ1 and the green fluorescent protein (GFP) (28) and membrane-targeted GFP were provided by Professor Tobias Meyer (Stanford University, Stanford, CA).

Cell culture and transfection. MIN6 β-cells (29) of passages 17–32 were cultured in Dulbecco's modified Eagle's medium containing 25 mmol/l glucose and supplemented with 2 mmol/l glutamine, 70 μmol/l 2-mercaptoethanol, 100 units/ml penicillin, 100 μg/ml streptomycin, and 15% fetal calf serum. After plating onto 25-mm coverslips at a density of 1.5×10^5/ml, the cells were transiently transfected with 2 μg of plasmid DNA and Lipofectamine 2000 (Invitrogen, Carlsbad, CA) in a 1:2.5 DNA:lipid ratio according to the manufacturer's protocol and further cultured for 12–24 h.

Buffers and permeabilization. Before experiments, the cells were transferred to a buffer containing 125 mmol/l NaCl, 4.8 mmol/l KCl, 1.3 mmol/l $CaCl_2$, 1.2 mmol/l $MgCl_2$, and 25 mmol/l HEPES with pH adjusted to 7.40 with NaOH. For $[Ca^{2+}]_i$ measurements, transfected cells were loaded with the Ca^{2+} indicator Fura Red by 30 min incubation at 37°C with 10 μmol/l of its acetoxymethyl ester (Molecular Probes, Eugene, OR).

In some experiments, the cells were permeabilized with Staphylococcal α-toxin (PhPlate Stockholm, Stockholm, Sweden). Before permeabilization the cells were superfused with an intracellular-like medium containing 140 mmol/l KCl, 6 mmol/l NaCl, 1 mmol/l $MgCl_2$, 2 mmol/l EGTA, 0.465 mmol/l $CaCl_2$, and 10 mmol/l HEPES with pH adjusted to 7.00 with KOH. Temporarily interrupting the perfusion, 5 μl α-toxin (0.46 mg/ml) was added directly into the 50-μl superfusion chamber. After permeabilization, 0.025–3 mmol/l MgATP was added to the medium. Free Ca^{2+} was buffered to 100 nmol/l using 2 mmol/l EGTA.

Fluorescence microscopy. The coverslips with the attached cells were used as exchangeable bottoms of the 50-μl open chamber and superfused at a rate of 0.3 ml/min. All experiments were performed at 37°C. Plasma membrane concentrations of the fluorescent protein constructs were measured using an evanescent wave microscopy setup as previously described (16). Selection of excitation and emission wavelengths were made with the following filters (center wavelength/half-bandwidth nm): GFP, excitation 488/10 nm and emission 525/25 nm; Fura Red, excitation 488/10 nm and emission 630 nm long pass. Images or image pairs were acquired every 5 s. To minimize exposure to the potentially harmful laser light, the beam was blocked by an electronic shutter (Sutter Instruments, Novato, CA) between image captures.

Confocal imaging was performed with a Yokogawa CSU-10 spinning disk system (Andor Technology, Belfast, Northern Ireland) attached to a Diaphot 200 microscope (Nikon) equipped with a ×60 1.40 NA objective (Nikon). The 488-nm beam from an argon ion laser (Melles-Griot, Didam, the Netherlands) was coupled to the scan head through an optical fiber (Point-Source, Southampton, U.K.). Fluorescence was detected at 520/35 nm using an Orca-AG camera (Hamamatsu) under MetaFluor software control.

Data analysis. Image analysis was made with ImageJ software (W.S. Rasband, National Institutes of Health [http://rsb.info.nih.gov/ij]). Curve fitting was made with the Igor Pro software (Wavemetrics, Lake Oswego, OR). Fluorescent protein and Fura Red intensities are expressed as changes relative to initial fluorescence ($\Delta F/F_0$) after subtraction of background. Statistical analysis was performed using Student's t test. All data are presented as means ± SE.

RESULTS

Recording of plasma membrane PIP_2 concentration. Plasma membrane PIP_2 concentration was measured using the PIP_2- and IP_3-binding GFP-tagged PH domain from PLCδ1 ($PH_{PLCδ1}$-GFP). Conventional epifluorescence imaging revealed that the construct was predominantly located to the plasma membrane of unstimulated MIN6 β-cells maintained in buffer containing 3 mmol/l glucose (Fig. 1*A*). Selective illumination of the plasma membrane with evanescent wave microscopy demonstrated a homogenous fluorescence in the membrane area adhering to the coverslip (Fig. 1*A*). As previously reported (16,30), carbachol-stimulated hydrolysis of PIP_2 and generation of IP_3 via activation of PLC promoted loss of evanescent wave-excited fluorescence (Fig. 1*A* and *B*). This effect reflects the $PH_{PLCδ1}$-GFP dissociation from the membrane and binding to IP_3 in the cytoplasm. The translocation was rapidly reversed on removal of the stimulus (Fig. 1*B*).

Elevation of the glucose concentration from 3 to 11 mmol/l induced a small increase in evanescent wave-excited $PH_{PLCδ1}$-GFP fluorescence, reaching 4.9 ± 0.1% ($n = 27$) above basal level within <2 min of stimulation. This increase was followed by a more pronounced decline in fluorescence (9.2 ± 0.8%, $n = 23$) of variable duration, typically succeeded by a new increase and gradual stabilization to a steady level only slightly above baseline (Fig. 1*C*). The initial rise of $PH_{PLCδ1}$-GFP fluorescence most likely involved an effect on cell adhesion or cell volume rather than purely reflecting the PIP_2 concentration, because a similar rise was observed in cells expressing GFP in the cytoplasm (not shown) or targeted to the plasma membrane ($n = 13$; Fig. 1*D*). However, the pronounced glucose-induced decline and subsequent increase of $PH_{PLCδ1}$-GFP fluorescence had no counterpart in the control experiments, indicating that glucose stimulates hydrolysis and synthesis of plasma membrane PIP_2 in insulin-secreting cells.

Glucose-induced hydrolysis of membrane PIP_2 requires elevation of $[Ca^{2+}]_i$. Previous studies have indicated that glucose may stimulate PIP_2 hydrolysis either directly (13–15) or indirectly via elevation of $[Ca^{2+}]_i$ (11,12). We therefore investigated the temporal relationship between changes in $[Ca^{2+}]_i$ and PIP_2 during glucose stimulation of the MIN6 β-cells. Simultaneous recording of $[Ca^{2+}]_i$ with Fura Red and PIP_2 with $PH_{PLCδ1}$-GFP during elevation of the glucose concentration from 3 to 11 mmol/l demonstrated that the early reduction of $[Ca^{2+}]_i$, known to reflect stimulation of the sarco(endo)plasmic reticulum and plasma membrane Ca^{2+}-ATPases (31), was paralleled by the modest increase of $PH_{PLCδ1}$-GFP fluorescence, whereas the glucose-induced $[Ca^{2+}]_i$ elevation coincided with the drop of $PH_{PLCδ1}$-GFP fluorescence (Fig. 2*A*), most likely reflecting Ca^{2+}-mediated activation of PLC (15,16,30,32). From this experiment, it can also be seen that the $PH_{PLCδ1}$-GFP rapidly increases again when $[Ca^{2+}]_i$ drops ($t_{1/2} = 19 \pm 5$ s; $n = 22$), indicating an efficient resynthesis of PIP_2 and/or degradation of IP_3. Consistent with the idea that depolarization-induced elevation of $[Ca^{2+}]_i$ after closure of K_{ATP} channels in β-cells results in activation of PLC and a reduction of membrane PIP_2, it was found that 200 μmol/l of the K_{ATP} channel inhibitor tolbutamide induced a rapid

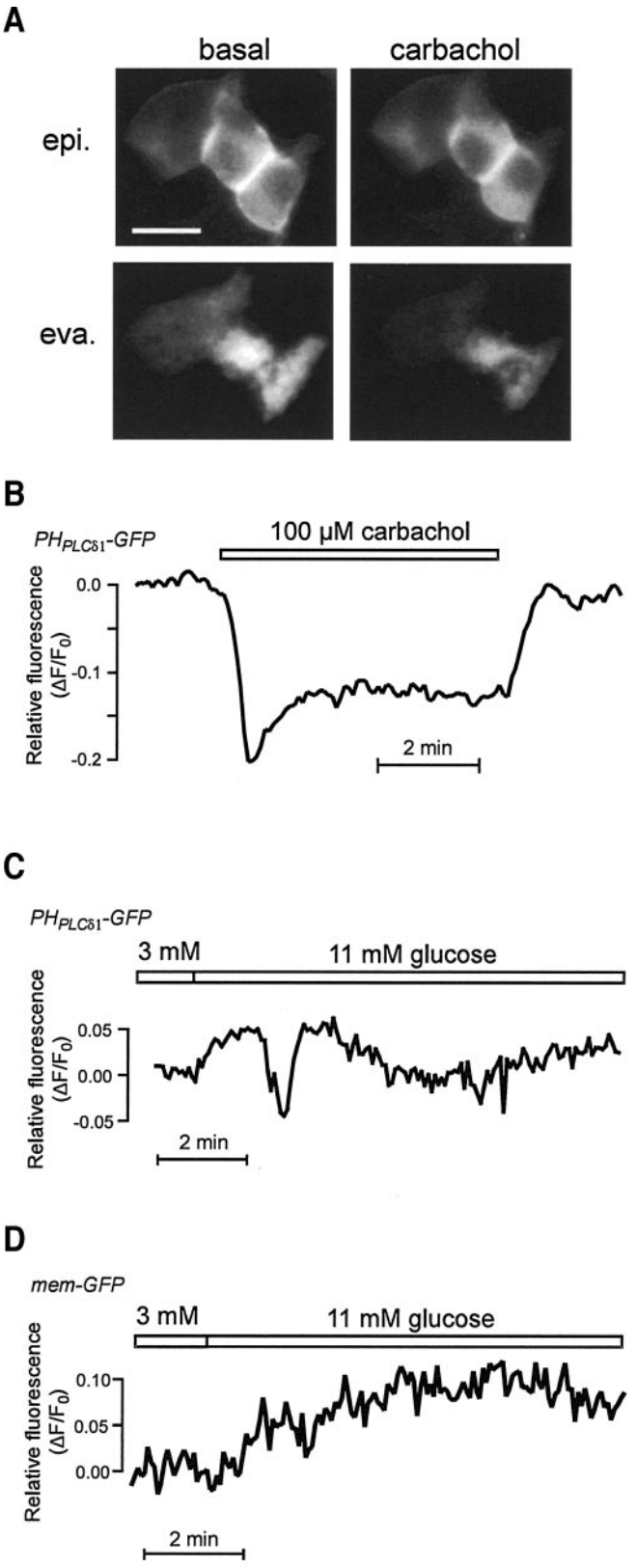

FIG. 1. Evanescent wave microscopy recording of plasma membrane PIP$_2$ concentration in individual cells. *A*: Epifluorescence (epi) and evanescent wave (eva) microscopy images of insulin-secreting MIN6 β-cells expressing the GFP-tagged PH domain from PLCδ1 (PH$_{PLC\delta1}$-GFP) under basal conditions and after stimulation with 100 μmol/l carbachol. Scale bar, 10 μm. *B* and *C*: Time course of PH$_{PLC\delta1}$-GFP translocation after stimulation with carbachol (*B*) or elevation of the glucose concentration from 3 to 11 mmol/l (*C*). *D*: Changes in fluorescence of membrane-targeted GFP during glucose stimulation. All traces are representative for at least 13 experiments.

elevation of $[Ca^{2+}]_i$ paralleled by a drop of membrane PH$_{PLC\delta1}$-GFP fluorescence (8.0 ± 1.2%, $n = 3$; Fig. 2*B*). Both changes of $[Ca^{2+}]_i$ and PH$_{PLC\delta1}$-GFP fluorescence were reversed on washout of the drug. Some cells responded to elevation of the glucose concentration with the β-cell characteristic oscillations of $[Ca^{2+}]_i$, reflecting periodic plasma membrane depolarization and Ca^{2+} influx (33). In this case, membrane PIP$_2$ concentration also varied in a periodic manner, with the nadirs in lipid concentration coinciding with increases of $[Ca^{2+}]_i$ and vice versa (Fig. 2*C*).

When the cells were stimulated with 11 mmol/l glucose in Ca^{2+}-deficient medium containing 2 mmol/l EGTA, there was an early reduction but no subsequent increase of $[Ca^{2+}]_i$. Under this condition, glucose triggered a monophasic rise of PH$_{PLC\delta1}$-GFP fluorescence to a level significantly above that obtained in the presence of extracellular Ca^{2+} (9.4 ± 2.1%, $n = 6$ vs. 2.5 ± 1%, $n = 27$; $P < 0.01$; data not shown). Similarly, when voltage-dependent Ca^{2+} influx was prevented by 250 μmol/l of the hyperpolarizing agent diazoxide, glucose triggered a modest decrease of $[Ca^{2+}]_i$ that was paralleled by a pronounced increase of PH$_{PLC\delta1}$-GFP fluorescence reaching steady state at 8.3 ± 1.1% above baseline ($n = 30$; Fig. 2*D*). Subsequent omission of diazoxide resulted in elevation of $[Ca^{2+}]_i$ and a rapid drop of PH$_{PLC\delta1}$-GFP fluorescence (Fig. 2*D*). Taken together, these results show that glucose promotes breakdown of PIP$_2$ in the plasma membrane of single insulin-secreting cells via elevation of $[Ca^{2+}]_i$ and that the lipid undergoes rapid resynthesis after termination of the $[Ca^{2+}]_i$ signal.

Plasma membrane PIP$_2$ undergoes rapid turnover. The regulation of plasma membrane PIP$_2$ concentration was further characterized in individual MIN6 β-cells permeabilized with α-toxin from *Staphylococcus aureus*. The pores formed in the plasma membrane by this toxin allow passage of molecules up to ~1 kDa (34). Thus, small molecules, such as ions and nucleotides, can permeate, whereas most proteins, including the PH$_{PLC\delta1}$-GFP probe, remain inside the cell. Permeabilization of PH$_{PLC\delta1}$-GFP–expressing MIN6 β-cells in an ATP-free intracellular-like medium resulted in loss of evanescent wave-excited membrane PH$_{PLC\delta1}$-GFP fluorescence. Confocal microscopy revealed that the probe was localized predominantly to the cytoplasm under this condition (Fig. 3*A*). Introduction of 3 mmol/l ATP resulted in a rapid ($t_{1/2} = 16 \pm 1$ s, $n = 32$) and prominent (131 ± 10%, $n = 32$) increase of evanescent wave-excited membrane PH$_{PLC\delta1}$-GFP fluorescence (Fig. 3*A* and *B*). The effect was reversed on removal of ATP ($t_{1/2} = 39 \pm 5$ s, $n = 32$; Fig. 3*B*), likely reflecting lipid phosphatase activity. Reintroduction of ATP caused a new increase of fluorescence, albeit with somewhat lower amplitude (76 ± 5% of that of first pulse, $n = 7$; Fig. 3*B*). The effect of ATP on PH$_{PLC\delta1}$-GFP fluorescence was completely abolished by 100 μmol/l phenylarsine oxide, a PI 4-kinase inhibitor ($n = 7$; Fig. 3*C*). ATP was also without effect in cells expressing GFP alone targeted to the plasma membrane ($n = 4$; Fig. 3*D*), indicating that the changes in PH$_{PLC\delta1}$-GFP fluorescence reflected changes in membrane PIP$_2$ concentration.

We next investigated the ATP dependence of PIP$_2$ synthesis in permeabilized MIN6 β-cells. Application of increasing concentrations of ATP from 25 μmol/l to 3 mmol/l resulted in graded increases of membrane PIP$_2$ concentration (Fig. 4*A*). Half-maximal and maximal stimulatory effects were obtained at ~300 μmol/l and ~1 mmol/l of the nucleotide, respectively (Fig. 4*B*). The

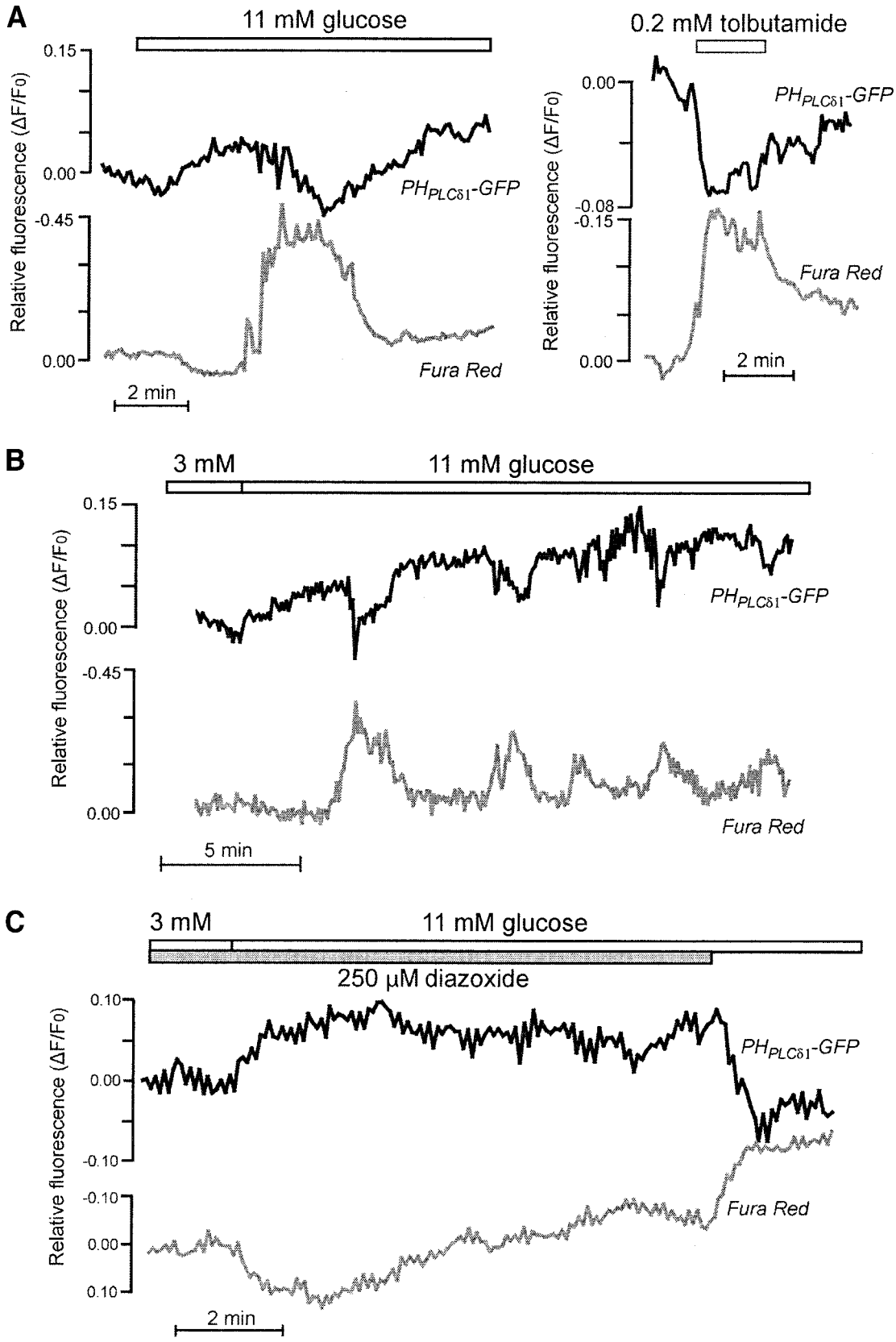

FIG. 2. Glucose-induced hydrolysis of membrane PIP_2 requires elevation of $[Ca^{2+}]_i$. *A*: Simultaneous evanescent wave microscopy recordings of membrane PIP_2 with $PH_{PLC\delta1}$-GFP and $[Ca^{2+}]_i$ with Fura Red during elevation of the glucose concentration from 3 to 11 mmol/l (n = 27). *B*: Effect of 0.2 mmol/l tolbutamide (n = 3). *C*: Glucose-induced oscillations of $[Ca^{2+}]_i$ and membrane PIP_2 concentration (n = 5). *D*: Effect of glucose in the presence of 250 μmol/l diazoxide (n = 30). The Fura Red traces have been inverted to show $[Ca^{2+}]_i$ increases as upward deflections.

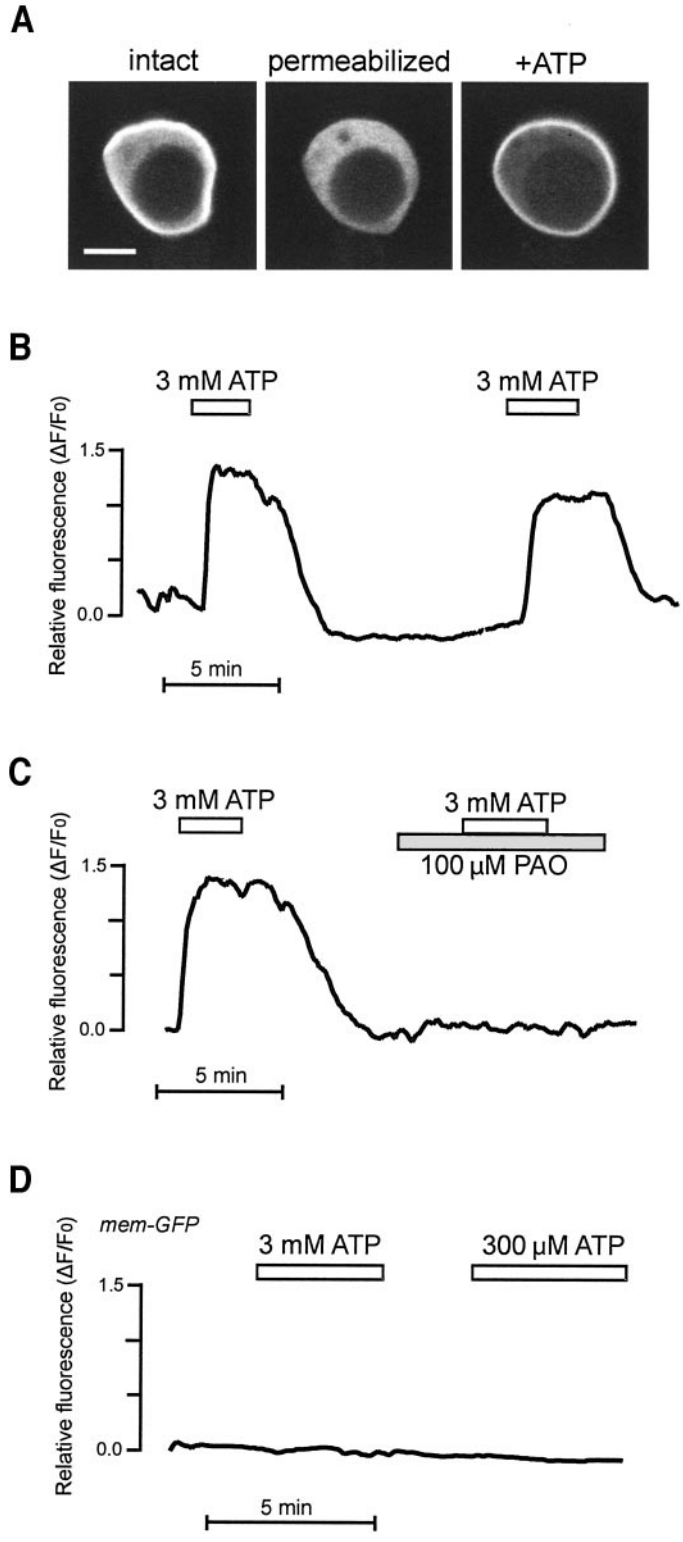

FIG. 3. Measurement of membrane PIP$_2$ concentration in individual permeabilized insulin-secreting cells. *A*: Confocal microscopy images of a MIN6 β-cell expressing PH$_{PLC\delta1}$-GFP before and after α-toxin permeabilization in an "intracellular" medium lacking ATP and after subsequent introduction of 3 mmol/l ATP. Scale bar, 5 μm. *B*: Evanescent wave microscopy recording of the effect of 3 mmol/l ATP on PH$_{PLC\delta1}$-GFP fluorescence in an individual permeabilized MIN6 β-cell (n = 7). *C*: Effect of 100 μmol/l phenylarsine oxide (PAO) on the ATP-induced PH$_{PLC\delta1}$-GFP translocation (n = 7). *D*: Effect of ATP on membrane-targeted GFP in a permeabilized MIN6 β-cell (n = 4).

concentration dependence was strikingly steep with a Hill coefficient of 9.7. This value may be overestimated because of the gradual desensitization of the response during repeated or prolonged exposure to ATP. In contrast, the results were not skewed by PLC activation via purinergic receptors, because 5 μmol/l of the PLC inhibitor U73122 was without effect on the PH$_{PLC\delta1}$-GFP fluorescence level reached with 300 μmol/l ATP (n = 6; Fig. 4*C*). At 300 μmol/l ATP the $t_{1/2}$ for PIP$_2$ synthesis averaged 49 ± 5 s (n = 29) and that for breakdown on removal of ATP 16 ± 2 s (n = 12), demonstrating high turnover of PIP$_2$ in the plasma membrane. Inositol availability was not rate limiting for PIP$_2$ synthesis on a short time scale as addition of 0.5 mmol/l *myo*-inositol was without effect on the steady-state level (n = 7; data not shown). Nevertheless, a fraction of the PIP$_2$ synthesis may require de novo generation of phosphatidylinositol, because 10 mmol/l Li^+, which prevents inositol recycling from inositolmonophosphate (35), suppressed the steady-state PH$_{PLC\delta1}$-GFP fluorescence level by 16.5 ± 2.9% (n = 9; Fig. 4*D*). Together, the data suggest that PIP$_2$ turnover essentially reflects a cycle of rapid phosphorylation of PI to PIP and PIP$_2$ and dephosphorylation back to PIP and PI.

Plasma membrane PIP$_2$ concentration is determined by the ATP-to-ADP ratio. Many processes in β-cells are regulated by the ratio of ATP to ADP rather than by the ATP concentration itself (36). We therefore investigated the influence of ADP on PIP$_2$ synthesis in the permeabilized MIN6 cells. Unexpectedly, application of ADP alone resulted in prompt stimulation of PIP$_2$ synthesis (Fig. 5*A*). This effect probably reflects adenylate kinase–catalyzed formation of ATP from ADP (37), because it was prevented by 25 μmol/l P^1,P^5-di(adenosine-5′) pentaphosphate, an adenylate kinase inhibitor (Fig. 5*A*). To circumvent this complication, we made use of the ADP analog adenosine-5′-*O*-2-thiodiphosphate (ADPβS), which is not a substrate for adenylate kinase (38). In the absence of ATP, 0.1–1 mmol/l ADPβS was without effect on PH$_{PLC\delta1}$-GFP fluorescence. However, the ADP analog counteracted ATP-stimulated PIP$_2$ synthesis. Thus, in the presence of 1 mmol/l ADPβS, the increase of PH$_{PLC\delta1}$-GFP fluorescence after stimulation with 500 μmol/l ATP reached only 49.5 ± 6.3% of that in controls (n = 9; P < 0.001; Fig. 5*B* and *C*). PIP$_2$ synthesis was significantly stimulated by subsequent reduction of the ADPβS concentration to 100 μmol/l with PH$_{PLC\delta1}$-GFP fluorescence reaching 80.2 ± 7.3% of that obtained in the absence of ADP analog (n = 9, P < 0.02; Fig. 5*C* and *D*). Similarly, introduction of increasing concentrations of ADPβS in the continuous presence of 300 μmol/l ATP caused a dose-dependent loss of fluorescence (Fig. 5*D* and *E*). When the relative PH$_{PLC\delta1}$-GFP fluorescence was plotted against the ATP-to-ADPβS ratio, there was a clear sigmoidal relationship with half-maximum at a ratio of 0.74 and a Hill coefficient of 0.90 (Fig. 5*F*). These data indicate that changes of the ATP-to-ADP ratio in the physiological range (~2–10) (39) can regulate the membrane PIP$_2$ concentration in insulin-secreting cells from ~70 to 90% of maximum.

DISCUSSION

In the present study, we characterized the regulation of the plasma membrane PIP$_2$ concentration in individual MIN6 β-cells using the PH domain from PLCδ, a well-established tool that has provided important insights into the regulation of PLC activity in various types of cells

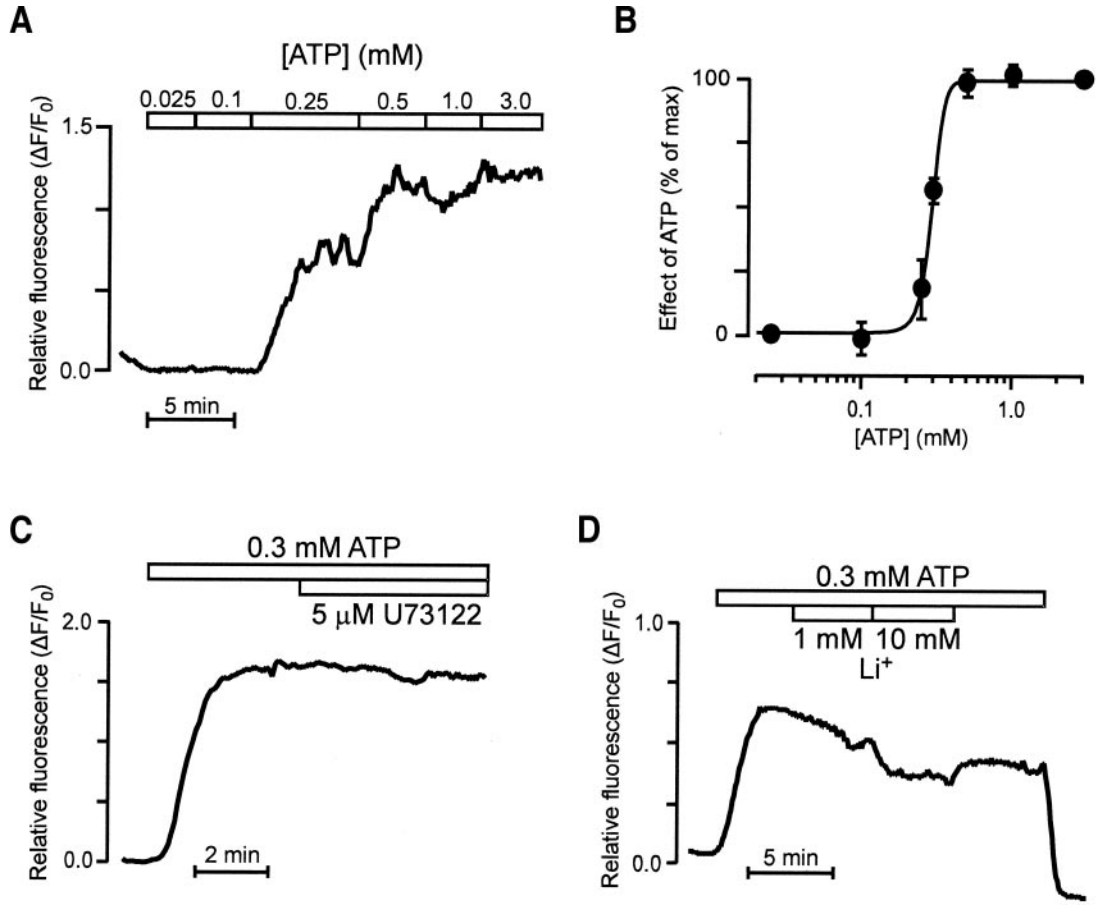

FIG. 4. Characterization of ATP-dependent plasma membrane PIP_2 synthesis. *A*: Evanescent wave microscopy recording of the effect of increasing concentrations of ATP on $PH_{PLC\delta1}$-GFP fluorescence in an individual α-toxin permeabilized MIN6 β-cell (n = 6). *B*: Concentration dependence of the ATP-induced $PH_{PLC\delta1}$-GFP translocation. The data points are fitted to a Hill equation. *C*: Effect of the PLC inhibitor U73122 on $PH_{PLC\delta1}$-GFP fluorescence (n = 6). *D*: Effect of 1 and 10 mmol/l Li^+ on ATP-stimulated $PH_{PLC\delta1}$-GFP translocation (n = 9).

(16,17,28,30,40). Glucose was found to trigger Ca^{2+}-dependent hydrolysis of PIP_2 via PLC. We also determined the requirements for intracellular adenine nucleotides for the synthesis of the lipid. The data indicate that PIP_2 undergoes rapid turnover in the plasma membrane and that its concentration is controlled by the intracellular ATP-to-ADP ratio.

Glucose stimulation of pancreatic β-cells is associated with voltage-gated influx of Ca^{2+}, which triggers exocytosis of insulin granules. We now observed that the glucose-induced rise of $[Ca^{2+}]_i$ is associated with loss of membrane PIP_2, an effect that can be attributed to Ca^{2+}-dependent activation of PLC. It has previously been shown (16,17,30) that this enzyme is tightly and dynamically regulated by $[Ca^{2+}]_i$ and that depolarization and influx of Ca^{2+} independently trigger PLC activation in insulin-secreting cells (16). Accordingly, depolarization with the K_{ATP} channel inhibitor tolbutamide was found to cause both rise of $[Ca^{2+}]_i$ and loss of membrane PIP_2 and glucose-induced oscillations of $[Ca^{2+}]_i$ paralleled by oscillations of PIP_2. Furthermore, the glucose-induced loss of PIP_2 was abolished when Ca^{2+} influx was prevented by the hyperpolarizing agent diazoxide or by removal of extracellular Ca^{2+}. These data reinforce the idea that glucose stimulation of β-cells leads to IP_3 formation via Ca^{2+}-dependent activation of PLC. Periodic formation of IP_3 may contribute to the generation and shaping of the oscillations of membrane potential and $[Ca^{2+}]_i$ in insulin-secreting cells (33,41,42).

It is likely that glucose, apart from stimulating hydrolysis of PIP_2, also stimulates the synthesis of the lipid. It was recently suggested that glucose stimulates synthesis of PIP and PIP_2 via activation of the Ca^{2+}-binding protein neuronal calcium sensor-1 and PI 4-kinase type IIIβ in INS1-E cells (43). Such an effect may escape detection in our system. The glucose-induced unspecific increase of plasma membrane fluorescence could mask a modest rise of PIP_2 concentration. Moreover, the higher affinity of the PLCδ PH domain for IP_3 compared with PIP_2 (44) may result in underestimation of the PIP_2 concentration in the presence of elevated $[Ca^{2+}]_i$. To circumvent the potential problem of determining whether the observed kinetics represents changes in PIP_2 or IP_3 concentration, we now made use of permeabilized cells where any formed IP_3 rapidly will be washed away. The remaining $PH_{PLC\delta1}$-GFP signal therefore reflects PIP_2 concentration changes in the plasma membrane. This conclusion is supported by the observation that ATP stimulated an increase of fluorescence that was abolished by inhibition of PI 4-kinases. Our novel experimental approach demonstrated that PIP_2 undergoes rapid turnover with a half-life of $<$40 s and provides direct support for the early observation that the plasma membrane lipid phosphatidylinositol undergoes futile cycles of continuous phosphorylation to PIP and PIP_2 and dephosphorylation to PIP and PI (1). Although metabolically expensive, a high turnover is a prerequisite for a messenger molecule to undergo rapid changes in

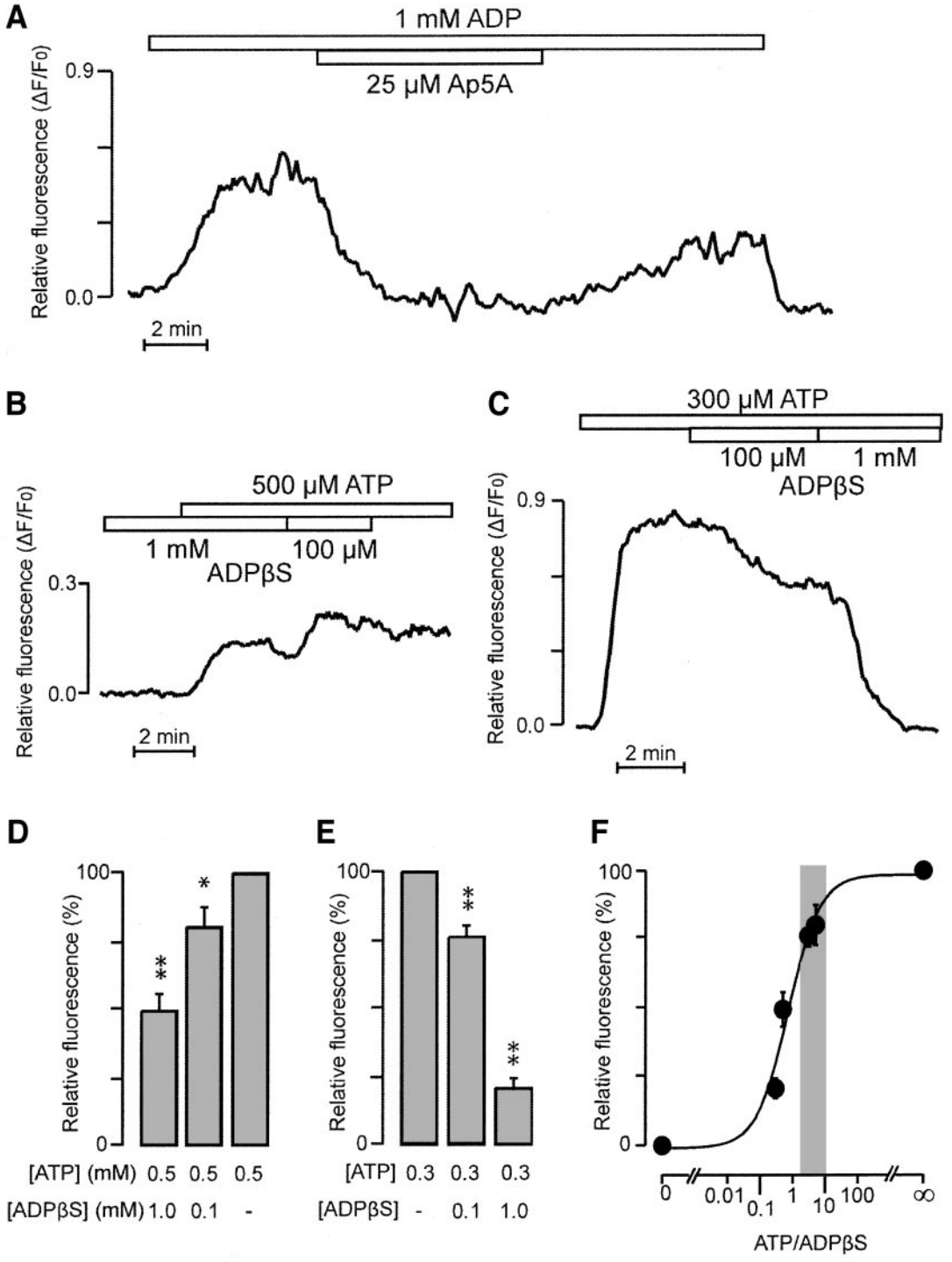

FIG. 5. Plasma membrane PIP$_2$ concentration is regulated by the intracellular ATP-to-ADP ratio. *A*: Evanescent wave microscopy recording of the effect of ADP and the adenylate kinase inhibitor diadenosine pentaphosphate (Ap5A) on PH$_{PLC\delta1}$-GFP fluorescence in an individual α-toxin permeabilized MIN6 β-cell (n = 7). *B* and *C*: PH$_{PLC\delta1}$-GFP translocation in the presence of different concentrations of ATP and ADPβS. Data are representative of 11 (*B*) and 9 (*C*) cells. *D* and *E*: Averages ± SE for the effect of ADPβS on PH$_{PLC\delta1}$-GFP fluorescence. *P < 0.02; **P < 0.001 for difference from 100%. *F*: Dependence of the PH$_{PLC\delta1}$-GFP translocation on the ATP-to-ADPβS ratio. The data points are fitted to a Hill equation. The shaded rectangle represents the physiological range of ratios.

concentration or to maintain concentration gradients in spatially restricted domains.

The synthesis of membrane PIP$_2$ was half-maximally stimulated at ~300 μmol/l ATP, a concentration that compares favorably with previous reports based on biochemical characterization of phosphoinositide kinases (45). Although this sensitivity seems too high to enable regulation of PIP$_2$ synthesis by changes in the cytoplasmic concentration of ATP, which is in the low millimolar range, this possibility should not be excluded. The situation is reminiscent of that for the K_{ATP} channel, which is regulated by changes in cytoplasmic adenine nucleotides, although the channel is completely inhibited by micromolar concentrations of ATP in isolated membrane patches

(46). In the case of the K_{ATP} channel, the action of ATP is counteracted by ADP, which may be formed locally by ATP hydrolysis (46) or phosphotransfer mediated by adenylate kinase (47). Interestingly, our data show that adenylate kinase has a functional effect also on adenine nucleotide–mediated PIP_2 synthesis. The glucose-induced formation of ATP occurs at the expense of ADP, which results in an increase of the ATP-to-ADP ratio in the β-cell. Changes in this ratio are important for regulating secretion, not only by modulating the conductance of K_{ATP} channels but also by altering amplifying pathways for insulin release (7). Our finding that the plasma membrane PIP_2 concentration has a very steep ATP dependence and is negatively regulated by an ADP analog supports the idea that PIP_2 synthesis in pancreatic β-cells, driven by stimulated metabolism, may be controlled by the ATP-to-ADP ratio rather than by ATP alone. A similar conclusion was reached using mouse pancreatic islets and an in vitro kinase assay (25). Such an effect may be mediated by direct nucleotide regulation of phosphoinositide kinase activity (48). Future studies will determine which phosphoinositide kinase isoforms and regulatory mechanisms account for PIP_2 synthesis in insulin-secreting cells.

Because PIP_2 is capable of regulating many targets in the vicinity of the plasma membrane, it is likely that the high turnover of the lipid in glucose-stimulated β-cells will influence proteins involved in the regulation of insulin secretion. Moreover, rapid turnover of PIP_2 allows generation of second messengers with maintenance of adequate levels of PIP_2 critical for sustained insulin granule exocytosis. It is interesting to note that impaired synthesis of PIP_2 with lower concentration of the lipid has been reported in an animal model of type 2 diabetes with insufficient insulin secretion (49).

ACKNOWLEDGMENTS

This work was supported by grants from Åke Wiberg's Foundation, the European Foundation for the Study of Diabetes/MSD, the Family Ernfors Foundation, the Harald Jeansson's and Harald and Greta Jeansson's Foundations, the Novo Nordisk Foundation, the Swedish Diabetes Association, the Swedish Research Council (32X-14643, 32BI-15333, and 32P-15439), and the Wenner-Gren Foundations.

REFERENCES

1. Berridge MJ, Irvine RF: Inositol trisphosphate, a novel second messenger in cellular signal transduction. *Nature* 312:315–321, 1984
2. Cantley LC: The phosphoinositide 3-kinase pathway. *Science* 296:1655–1657, 2002
3. Hilgemann DW, Feng S, Nasuhoglu C: The complex and intriguing lives of PIP_2 with ion channels and transporters. *Sci STKE* 2001:RE19, 2001
4. van Rheenen J, Jalink K: Agonist-induced PIP_2 hydrolysis inhibits cortical actin dynamics: regulation at a global but not at a micrometer scale. *Mol Biol Cell* 13:3257–3267, 2002
5. Martin TF: $PI(4,5)P_2$ regulation of surface membrane traffic. *Curr Opin Cell Biol* 13:493–499, 2001
6. Fruman DA, Meyers RE, Cantley LC: Phosphoinositide kinases. *Annu Rev Biochem* 67:481–507, 1998
7. Henquin JC: Triggering and amplifying pathways of regulation of insulin secretion by glucose. *Diabetes* 49:1751–1760, 2000
8. Clements RS Jr, Rhoten WB: Phosphoinositide metabolism and insulin secretion from isolated rat pancreatic islets. *J Clin Invest* 57:684–691, 1976
9. Laychock SG: Identification and metabolism of polyphosphoinositides in isolated islets of Langerhans. *Biochem J* 216:101–106, 1983
10. Morgan NG, Montague W: Phospholipids and insulin secretion. In *Nutrient Regulation of Insulin Secretion*. Flatt PR, Ed. London, Portland Press, 1992, p. 125–155
11. Clements RS Jr, Evans MH, Pace CS: Substrate requirements for the phosphoinositide response in rat pancreatic islets. *Biochim Biophys Acta* 674:1–9, 1981
12. Axen KV, Schubart UK, Blake AD, Fleischer N: Role of Ca^{2+} in secretagogue-stimulated breakdown of phosphatidylinositol in rat pancreatic islets. *J Clin Invest* 72:13–21, 1983
13. Best L, Malaisse WJ: Stimulation of phosphoinositide breakdown in rat pancreatic islets by glucose and carbamylcholine. *Biochem Biophys Res Commun* 116:9–16, 1983
14. Dunlop ME, Larkins RG: The role of calcium in phospholipid turnover following glucose stimulation in neonatal rat cultured islets. *J Biol Chem* 259:8407–8411, 1984
15. Biden TJ, Peter-Riesch B, Schlegel W, Wollheim CB: Ca^{2+}-mediated generation of inositol 1,4,5-triphosphate and inositol 1,3,4,5-tetrakisphosphate in pancreatic islets: studies with K^+, glucose, and carbamylcholine. *J Biol Chem* 262:3567–3571, 1987
16. Thore S, Dyachok O, Tengholm A: Oscillations of phospholipase C activity triggered by depolarization and Ca^{2+} influx in insulin-secreting cells. *J Biol Chem* 279:19396–19400, 2004
17. Tamarina NA, Kuznetsov A, Rhodes CJ, Bindokas VP, Philipson LH: Inositol (1,4,5)-trisphosphate dynamics and intracellular calcium oscillations in pancreatic β-cells. *Diabetes* 54:3073–3081, 2005
18. Hay JC, Martin TF: Phosphatidylinositol transfer protein required for ATP-dependent priming of Ca^{2+}-activated secretion. *Nature* 366:572–575, 1993
19. Hay JC, Fisette PL, Jenkins GH, Fukami K, Takenawa T, Anderson RA, Martin TF: ATP-dependent inositide phosphorylation required for Ca^{2+}-activated secretion. *Nature* 374:173–177, 1995
20. Wiedemann C, Schäfer T, Burger MM: Chromaffin granule-associated phosphatidylinositol 4-kinase activity is required for stimulated secretion. *EMBO J* 15:2094–2101, 1996
21. Gong LW, Di Paolo G, Diaz E, Cestra G, Diaz ME, Lindau M, De Camilli P, Toomre D: Phosphatidylinositol phosphate kinase type I gamma regulates dynamics of large dense-core vesicle fusion. *Proc Natl Acad Sci U S A* 102:5204–5209, 2005
22. Lawrence JT, Birnbaum MJ: ADP-ribosylation factor 6 regulates insulin secretion through plasma membrane phosphatidylinositol 4,5-bisphosphate. *Proc Natl Acad Sci U S A* 100:13320–13325, 2003
23. Waselle L, Gerona RR, Vitale N, Martin TF, Bader MF, Regazzi R: Role of phosphoinositide signaling in the control of insulin exocytosis. *Mol Endocrinol* 19:3097–3106, 2005
24. Holz RW, Hlubek MD, Sorensen SD, Fisher SK, Balla T, Ozaki S, Prestwich GD, Stuenkel EL, Bittner MA: A pleckstrin homology domain specific for phosphatidylinositol 4, 5-bisphosphate (PtdIns-4,5-P_2) and fused to green fluorescent protein identifies plasma membrane PtdIns-4,5-P_2 as being important in exocytosis. *J Biol Chem* 275:17878–17885, 2000
25. Olsen HL, Høy M, Zhang W, Bertorello AM, Bokvist K, Capito K, Efanov AM, Meister B, Thams P, Yang SN, Rorsman P, Berggren PO, Gromada J: Phosphatidylinositol 4-kinase serves as a metabolic sensor and regulates priming of secretory granules in pancreatic β cells. *Proc Natl Acad Sci U S A* 100:5187–5192, 2003
26. Lin CW, Yan F, Shimamura S, Barg S, Shyng SL: Membrane phosphoinositides control insulin secretion through their effects on ATP-sensitive K^+ channel activity. *Diabetes* 54:2852–2858, 2005
27. Bittner MA, Holz RW: Phosphatidylinositol-4,5-bisphosphate: actin dynamics and the regulation of ATP-dependent and -independent secretion. *Mol Pharmacol* 67:1089–1098, 2005
28. Stauffer TP, Ahn S, Meyer T: Receptor-induced transient reduction in plasma membrane PtdIns(4,5)P_2 concentration monitored in living cells. *Curr Biol* 8:343–346, 1998
29. Miyazaki J, Araki K, Yamato E, Ikegami H, Asano T, Shibasaki Y, Oka Y, Yamamura K: Establishment of a pancreatic beta cell line that retains glucose-inducible insulin secretion: special reference to expression of glucose transporter isoforms. *Endocrinology* 127:126–132, 1990
30. Thore S, Dyachok O, Gylfe E, Tengholm A: Feedback activation of phospholipase C via intracellular mobilization and store-operated influx of Ca^{2+} in insulin-secreting β-cells. *J Cell Sci* 118:4463–4471, 2005
31. Gylfe E: Glucose-induced early changes in cytoplasmic calcium of pancreatic β-cells studied with time-sharing dual-wavelength fluorometry. *J Biol Chem* 263:5044–5048, 1988
32. Best L, Tomlinson S, Hawkins PT, Downes CP: Production of inositol trisphosphates and inositol tetrakisphosphate in stimulated pancreatic islets. *Biochim Biophys Acta* 927:112–116, 1987
33. Dryselius S, Grapengiesser E, Hellman B, Gylfe E: Voltage-dependent entry and generation of slow Ca^{2+} oscillations in glucose-stimulated pancreatic β-cells. *Am J Physiol* 276:E512–E518, 1999

34. Bhakdi S, Tranum-Jensen J: Alpha-toxin of *Staphylococcus aureus*. *Microbiol Rev* 55:733–751, 1991
35. Hallcher LM, Sherman WR: The effects of lithium ion and other agents on the activity of myo-inositol-1-phosphatase from bovine brain. *J Biol Chem* 255:10896–10901, 1980
36. Fridlyand LE, Ma L, Philipson LH: Adenine nucleotide regulation in pancreatic β-cells: modeling of ATP/ADP-Ca^{2+} interactions. *Am J Physiol Endocrinol Metab* 289:E839–E848, 2005
37. Dzeja PP, Terzic A: Phosphotransfer reactions in the regulation of ATP-sensitive K^+ channels. *FASEB J* 12:523–529, 1998
38. Gillespie PG, Hudspeth AJ: Adenine nucleoside diphosphates block adaptation of mechanoelectrical transduction in hair cells. *Proc Natl Acad Sci U S A* 90:2710–2714, 1993
39. Erecińska M, Bryla J, Michalik M, Meglasson MD, Nelson D: Energy metabolism in islets of Langerhans. *Biochim Biophys Acta* 1101:273–295, 1992
40. Varnai P, Balla T: Visualization of phosphoinositides that bind pleckstrin homology domains: calcium- and agonist-induced dynamic changes and relationship to myo-[^{3}H]inositol-labeled phosphoinositide pools. *J Cell Biol* 143:501–510, 1998
41. Fridlyand LE, Tamarina N, Philipson LH: Modeling of Ca^{2+} flux in pancreatic beta-cells: role of the plasma membrane and intracellular stores. *Am J Physiol Endocrinol Metab* 285:E138–E154, 2003
42. Ämmälä C, Larsson O, Berggren PO, Bokvist K, Juntti-Berggren L, Kindmark H, Rorsman P: Inositol trisphosphate-dependent periodic activation of a Ca^{2+}-activated K^+ conductance in glucose-stimulated pancreatic β-cells. *Nature* 353:849–852, 1991
43. Gromada J, Bark C, Smidt K, Efanov AM, Janson J, Mandic SA, Webb DL, Zhang W, Meister B, Jeromin A, Berggren PO: Neuronal calcium sensor-1 potentiates glucose-dependent exocytosis in pancreatic β cells through activation of phosphatidylinositol 4-kinase β. *Proc Natl Acad Sci U S A* 102:10303–10308, 2005
44. Lemmon MA, Ferguson KM, O'Brien R, Sigler PB, Schlessinger J: Specific and high-affinity binding of inositol phosphates to an isolated pleckstrin homology domain. *Proc Natl Acad Sci U S A* 92:10472–10476, 1995
45. Balla T: Phosphatidylinositol 4-kinases. *Biochim Biophys Acta* 1436:69–85, 1998
46. Tarasov AI, Girard CA, Ashcroft FM: ATP sensitivity of the ATP-sensitive K^+ channel in intact and permeabilized pancreatic β-cells. *Diabetes* 55:2446–2454, 2006
47. Schulze DU, Krippeit-Drews P, Düfer M, Janssen E, Wieringa B, Drews G: K_{ATP} channel activity in pancreatic beta cells is regulated by an adenylate kinase. *Diabetologia* 49 (Suppl. 1):301, 2006
48. Whitman M, Kaplan D, Roberts T, Cantley L: Evidence for two distinct phosphatidylinositol kinases in fibroblasts: implications for cellular regulation. *Biochem J* 247:165–174, 1987
49. Morin L, Giroix MH, Portha B: Decreased ATP-induced synthesis and Ca^{2+}-stimulated degradation of polyphosphoinositides in pancreatic islets from neonatally streptozotocin-diabetic rats. *Biochem Biophys Res Commun* 228:573–578, 1996